

Spectroscopic characterization of a single dangling bond on a bare Si(100)- $c(4 \times 2)$ surface for n - and p -type doping

M. Mantega,^{1,2} I. Rungger,^{1,2} B. Naydenov,^{1,3} J. J. Boland,^{1,3} and S. Sanvito^{1,2}¹*School of Physics, Trinity College, Dublin 2, Ireland*²*CRANN, Trinity College, Dublin 2, Ireland*³*School of Chemistry, Trinity College, Dublin 2, Ireland*

(Received 5 March 2012; revised manuscript received 19 June 2012; published 19 July 2012)

We investigate the charging state of an isolated single dangling bond formed on an unpassivated Si(100) surface with $c(4 \times 2)$ reconstruction, by comparing scanning tunneling microscopy and spectroscopy analysis with density functional theory calculations. The dangling bond is created by placing a single hydrogen atom on the bare surface with the tip of a scanning tunneling microscope. The H atom passivates one of the dimer dangling bonds responsible for the surface one-dimensional electronic structure. This leaves a second dangling at the reacted surface dimer which breaks the surface periodicity. We consider two possible H adsorption configurations for both the neutral and the doped situation (n - and p -type). In the case of n -doping we find that the single dangling bond state is doubly occupied and the most stable configuration is that with H bonded to the bottom Si atom of the surface dimer. In the case of p -doping the dangling bond is instead empty and the configuration with the H attached to the top atom of the dimer is the most stable. Importantly the two configurations have different scattering properties and phase shift fingerprints. This might open up interesting perspectives for fabricating a switching device by tuning the doping level or by locally charging the single dangling bond state.

DOI: [10.1103/PhysRevB.86.035318](https://doi.org/10.1103/PhysRevB.86.035318)

PACS number(s): 68.37.Ef, 61.72.uf, 68.43.-h, 71.15.Mb

I. INTRODUCTION

Despite the growing interest in novel materials platforms for implementing the next generation of nano-electronic devices, the Si(100) surface still remains the most important substrate for applications.^{1–6} Its high stability and the possibility of manipulating and functionalizing the surface properties at the atomic level are opening up new perspectives for a wide range of applications. These range from transistor downscaling, dictated by Moore's law, to quantum computing.^{7–10}

The adsorption of single atoms and small inorganic molecules is a key enabling tool for controlling the passivation, oxidation, and epitaxial growth of the surface. Hydrogen passivated Si(100), for example, can be patterned by desorbing H atoms with the tip of a scanning tunneling microscope (STM) and a variety of arrangements of coupled dangling bonds (quantum dots) can be created.^{11–15} While the electronic properties of a single dangling bond on an otherwise passivated surface are well understood, an exhaustive spectroscopic characterization of the charging state of the single dangling bond on a bare (unpassivated) Si(100) surface is lacking.

Previous reports on the STM characterization of H atoms on Si(100)^{16,17} have dealt with the room temperature imaging of low doped ($\sim 1 \Omega \text{ cm}$) n -type and high-doped ($\sim 0.004 \Omega \text{ cm}$) p -type samples. These have been corroborated by topography density functional theory (DFT) calculations using a $p(1 \times 2)$ reconstructed surface. Here we perform a thorough combined experimental and theoretical analysis of both the topographic and the spectroscopic properties of single dangling bonds on the Si(100) surface when the surface is in different doping states. In particular, we consider low resistivity samples ($\sim 0.003 \Omega \text{ cm}$ for both n - and p -doping) and low temperature measurements (77 K), a situation where the surface is found in a thermally stable $c(4 \times 2)$ reconstruction.^{18–20} In addition, to describing more precisely the isolated adsorbate by applying large unit cell (see below for details), we present its spatially

resolved electronic structure in the entire energy range from +1 to -1 V where all surface features are located.

In particular, scanning tunneling spectroscopy (STS) maps of the local density of states (LDOS) recovered from the dI/dV ²¹ are compared with the LDOS obtained from first-principles calculations to extract information about the charging state configurations of the single dangling bond (SDB). A SDB is created by placing a H atom on the dimer of a clean Si(100) surface with $c(4 \times 2)$ reconstruction. The adsorption of H can be performed by using an STM tip. The H atom passivates one of the two dangling bonds of the Si dimer, breaking the Si-Si dimer π bond and leaving an isolated dangling bond on the other site of the dimer.²² The type of electronic state originating from the SDB depends on whether the H atom sits on the top atom of the Si surface dimer, H_T , or on the bottom atom H_B . It also depends on the doping of the sample and on the surface strain. The two configurations, shown in Fig. 1, have been investigated for the intrinsic case (no doping) and for heavily n - and p -doped samples.

II. METHODS

First principles calculations are performed with the DFT VASP package,²³ using projected augmented wave (PAW) potentials together with the Perdew-Burke-Ernzerhof form of the generalized gradient approximation (PBE-GGA) to the exchange and correlation functional.^{24–26} The electronic properties of the $c(4 \times 2)$ reconstructed surface are calculated with a supercell and periodic boundary conditions. This contains 441 atoms arranged over 9 Si layers, one H passivating layer at the bottom of the cell and a 12 Å vacuum region at the top. Two rows of 10 alternating dimers form the topmost surface layer (see Fig. 1). The cutoff radius for the plane-waves expansion is set to 500 eV and a $3 \times 3 \times 1$ k -points mesh spans the Brillouin zone. Doping is introduced by adding

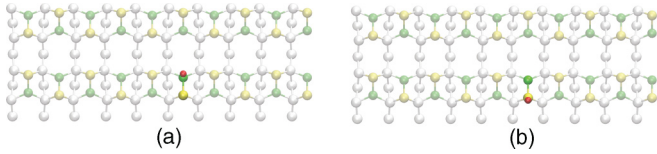


FIG. 1. (Color online) Top view (XY plane) of the H_B (a) and the H_T (b) configurations of a H atom (red) adsorbed on a clean Si(100) surface with $c(4 \times 2)$ reconstruction. Yellow and green atoms are, respectively, the top and bottom Si atoms of the dimerized topmost surface layer.

(or subtracting) one unit charge to the supercell and by compensating with a neutralizing uniform background. Due to the periodic boundary conditions, our system is equivalent to a quantum well where the H at the SDB site creates the potential barriers. The STM images have been simulated within the Tersoff-Hamann approximation^{27,28} by integrating the local DOS over an energy range around the Fermi level, E_F . The selected isosurface value corresponds to a distance of about 4 Å from the surface. This is a reasonable value considering the generally incorrect decay of the wave function in vacuum due to the incompleteness of the plane-wave basis set used and the erroneous asymptotic behavior of the GGA potential.

STM experiments are performed using a Createc cryogenic system described elsewhere.²¹ Both n -type (As, 0.001–0.005 Ω cm) and p -type (B, 0.001–0.005 Ω cm) Si(100) samples are used mounted on a triple sample holder containing also a Pt crystalline surface for tip preparation and characterization. *In situ* Pt-inked tungsten probe²⁹ is used in the STM. Sub-monolayer atomic hydrogen coverage is deposited on the clean surface at 200 K via heated tungsten capillary. The H atoms are manipulated by transferring them on and from the STM probe applying high biases (5–6 V) with different polarities. The spectroscopic results are obtained with variable-height scanning tunneling spectroscopy (VH-STs)²¹ at 77 K.

III. RESULTS AND DISCUSSION

We have shown before³⁰ that for heavily n -doped samples ($\rho \sim 0.001$ Ω cm), H_B is the most stable configuration. This is confirmed by DFT total energy calculations predicting H_B to be 136 meV lower in energy with respect to H_T for n -doping. The same feature is found in the neutral case although the energy difference between H_B and H_T becomes only 26 meV. Reusch *et al.* found comparable total energies for similar configurations¹⁶ and a similar trend was also found for Ge(001).³¹ By comparing the local density of state (LDOS) for the undoped and n -doped configurations it is possible to extract information about the charging state of the SDB. H_B on the neutral surface is characterized by a spin-polarized ground state with a localized spin split level at the SDB site. This gives a clear indication that such a state contains only one electron. The simulated LDOS as function of position along the dimer row and energy (in eV) is shown in Fig. 2, where the balls-and-sticks model indicates the position of the H atom and, consequently, of the SDB. Due to the periodic boundary conditions used here, the system is equivalent to a ~ 40 Å long quantum well with H atoms acting as potential barriers. The

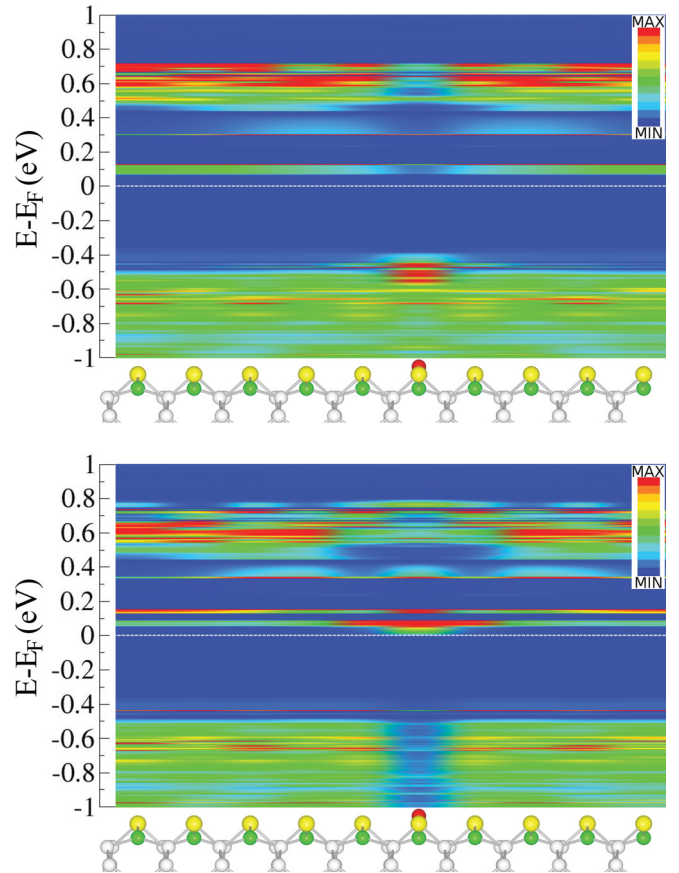


FIG. 2. (Color online) Calculated LDOS for H_B in the neutral case. The spin up (top panel) and spin down (bottom panel) states located at the SDB site can be found respectively at around 0.4 eV below E_F and 0.1 eV above E_F . Band bending here is negligible. The plot uses a color scale with blue meaning small DOS and red meaning the maximum DOS.

LDOS shows a partially filled spin up level 0.4 eV below E_F (see Fig. 2 top panel) and an empty spin down level at around 0.1 eV above E_F (see Fig. 2 bottom panel). Both these levels are localized at the site facing the H atom (see Fig. 3). The peak in the LDOS located at around 0.15 eV and present for both the spin channels is the first quantum well standing wave. In the minority spin channel this is partially hybridized with the state localized at the SDB site. Note that this is just an artifact of the periodic boundary conditions used for the calculations and it will not be discussed further.

When the surface is n -doped the ground state is no longer spin-polarized. The simulated DOS shows a single level at around 0.2 eV below E_F localized at the SDB site, suggesting that the SDB is doubly occupied (see Fig. 4 top panel). The band bending around the SDB site confirms this picture: the

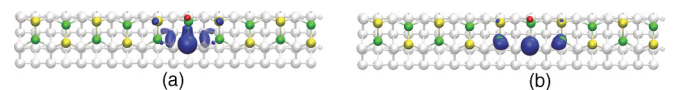


FIG. 3. (Color online) Charge density at the H_B site for the undoped surface: the first HOMO spin up (a) and the first LUMO spin down (b) level are localized at the SDB site.

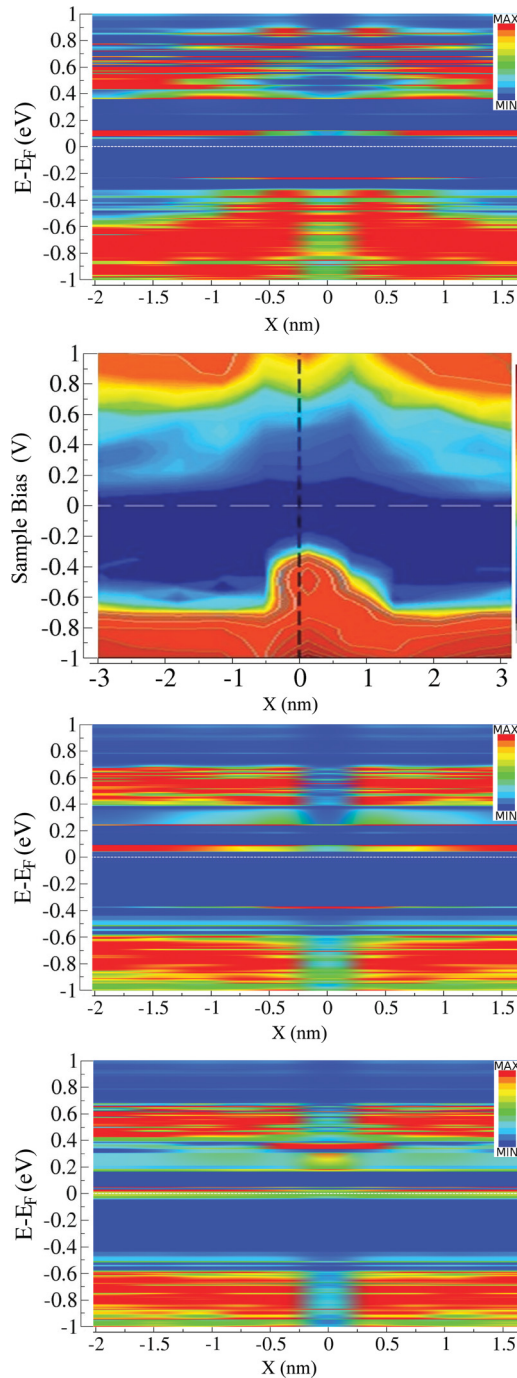


FIG. 4. (Color online) Calculated LDOS (top) for the n -doped H_B is compared with the experimental LDOS for the majority specie (second panel from the top). The SDB state is found to be at around 0.2 eV below E_F and it is doubly occupied. The spin-up and spin-down LDOS for the n -doped H_T is shown for completeness (respectively third and fourth panel from the top). The absence of band bending at the reacted site and the presence of spin-split delocalized states across E_F for H_T contrast the experimental finding (second panel) and allow us to attribute the binding site to H_B .

DOS in n -doping conditions reveals a pronounced upward band bending due to the extra charge while this is negligible for the undoped case, in very good agreement with our spectroscopic data (see Fig. 4, second panel from the top).

TABLE I. Total energy differences, buckling angles, and magnetic moments for different configurations.

Config.	Energy (meV)	H dimer (deg)	Magn. mom.
Bare surface		19.7	0
H_B	0	-0.106	0.95
H_T	+26	10.167	0
$H_B + 1e$	0	7.896	0
$H_T + 1e$	+136	2.279	0.79
$H_B - 1e$	0	-10.612	0
$H_T - 1e$	-111	11.198	0

Note that the calculated band curvature is more prominent than expected due to the periodic boundary conditions. The effect of the electrostatic repulsion due to the extra charge located at the SDB site is reflected in the structural properties of the system. The dimer bond length increases from 2.397 Å to 2.453 Å and the buckling angle goes from almost 0° to around 8° (see Table I for the structural data). When going from single to the double occupation the Si atom hosting the dangling bond changes its bonding configuration from a mixed sp^2 - sp^3 hybridization to a prevalent sp^3 character, i.e., the SDB has more s character.

Experimentally in n -doped samples we find the H_T configuration to appear with a frequency of less than 1% and it is thus defined as the minority specie. A negative bias causes the entire dimer row to flip to a H_B configuration so that only the positive bias region of the DOS (conduction band) is available.³⁰ Therefore, we will not discuss this case in detail. Still in Fig. 4 we present the calculated LDOS for the H_T configuration in n -doping conditions for majority and minority spins. The images denote a lack of band-bending and the presence of a spin-split delocalized states across

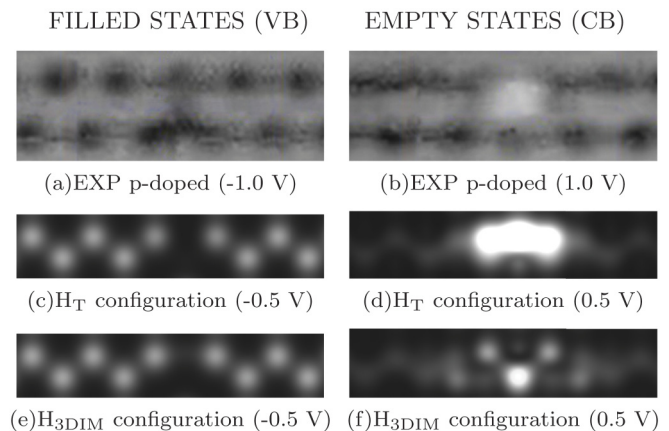


FIG. 5. Topographic images of H adsorbed on the Si(100) surface with $c(4 \times 2)$ reconstruction in p -doped conditions. The two top panels show the experimental topographies for filled (a) and empty (b) states acquired for a sample bias of -1.0 V and +1.0 V, respectively. These are compared with the calculated topographies for filled and empty states of the H_T [(c) and (d)], and H_{3DIM} [(e) and (f)] configurations. The simulated topographies are calculated using a bias of -0.5 V and +0.5 V, for filled and empty states, respectively. Note that only the H_T configuration matches the experimental topography in good agreement with calculated total energies.

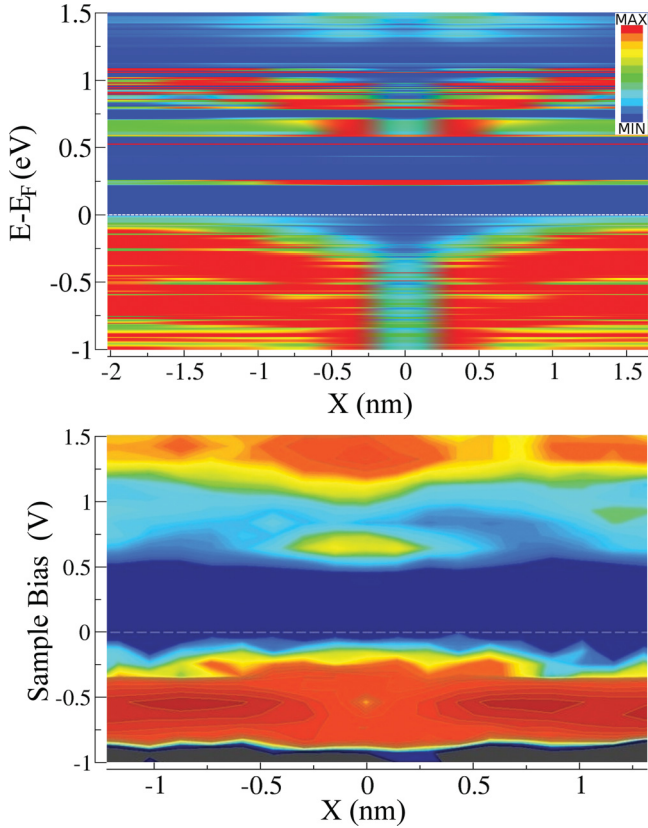


FIG. 6. (Color online) Calculated (top panel) and experimental (bottom panel) LDOS for p -doped H_T . In this case the single dangling bond state is empty as confirmed from the pronounced downward band bending.

E_F . These features are absent in the experimental STM spectra for the majority specie, which is then conclusive assigned to H_B .

Our calculations show the undoped H_T configuration having a non-spin-polarized ground state. The electron at the SDB state spreads along the neighboring dimers and gives rise to a level crossing E_F . The dimer buckling angle at the SDB site is $\sim 10^\circ$, suggesting that the bonding configuration of the Si atom hosting the dangling bond is sp^2 -like and the dangling bond is empty. These results are in good agreement with the HH2 antiparallel configuration described by Radny *et al.*, who found a buckling angle of 9.6° .¹⁷

We now move our attention to the p -doping situation. STM experiments of Si-Si-H hemihydrides on the Si(100) surface show the dangling bond appearing as a bright protrusion, while a depression is present on the opposite side of the dimer, for both filled and empty states.^{32,33} A comparison between the experimental and the computed topographic images for p -doped surfaces shows the H_T configuration to best match the data. In fact, although the simulated images for the filled states reveal that both H_T and H_B may agree with the experiments, only H_T reproduces the measured empty states topography (see Fig. 5). Our calculations show that, after a full relaxation, H_B undergoes an inversion in the dimer buckling, as reported in Table I. Such a new relaxed structure, called hereafter H_{3DIM} ,

presents the reacted dimer tilted in phase relative to its nearest neighbors. Total energy calculations predict H_T to be 111 meV lower than H_{3DIM} in good agreement with an energy difference of 140 meV previously reported.¹⁶ This energy difference is mostly due to the structural distortion induced by the H_{3DIM} configuration, which is less efficient in accommodating the surface strain. This configuration has never been observed experimentally.

STS data and calculated local DOS are in a good agreement and establish that the single dangling bond state is empty (Fig. 6).

This is confirmed by a pronounced downward band bending which is expected due to the positive charge around the SDB site (Fig. 6). The SDB state appears as a bright red spot around 0.2 eV above E_F for the calculated LDOS (see Fig. 6 top panel) and around 0.5 eV in experiments (see Fig. 6 bottom panel) at a spatial position corresponding to the H site. The buckling angle of $\sim 11^\circ$ suggests that the bonding configuration of Si atom at the SDB site is sp^2 -like, due to the absence of electrons at the SDB state.

IV. CONCLUSIONS

In conclusion, DFT calculations together with STM/STS experiments allowed us to unequivocally characterize the geometry and the charging state of SDB on the Si(100) surface in different doping conditions. For n -doping the H-produced SDB is double occupied with the H_B configuration being the lowest in energy. This configuration coincides with the majority specie found in low temperature STM experiments. For p -doped samples the H_T configuration is the lowest in energy and the SDB state is empty. Finally, according to our calculations, the SDB state is partially occupied and spin-polarized for the intrinsic neutral case. The buckling angle of the reacted dimer and, correspondingly, the bonding character of the Si atoms at SDB site reflects the occupation of the SDB state: (i) an sp^3 -like symmetry is found when the SDB is doubly occupied; (2) an sp^2 -like symmetry corresponds to an empty SDB state; (3) a hybrid configuration in between the two is found for a partial occupation (one electron in the SDB state). Such an interplay between charging and geometry might open the interesting prospective of fabricating an atomic-scale switching device. In fact by tuning the surface doping from p -type to n -type one may switch between the two H configurations. These have distinct scattering and transport properties,³⁰ so that the switch can be detected electrically.

ACKNOWLEDGMENTS

We would like to acknowledge the Trinity Centre for High Performance Computing (TCHPC) and the Irish Center for High-End Computing (ICHEC) for computational resources. Funding has been provided by Science Foundation Ireland (Grants No. 07/IN.1/1945 and No. 06/IN.1/1106) and the King Abdullah University of Science and Technology (ACRAB project).

- ¹K. S. Novoselov, A. K. Geim, S. V. Morozov, D. Jiang, Y. Zhang, S. V. Dubonos, I. V. Grigorieva, and A. A. Firsov, *Science* **306**, 666 (2004).
- ²M. C. Lemme, T. J. Echtermeyer, M. Baus, and H. Kurz, *IEEE Electron Device Lett.* **28**, 282 (2007).
- ³R. Sordan, F. Traversi, and V. Russo, *Appl. Phys. Lett.* **94**, 073305 (2009).
- ⁴Y. M. Lin, C. Dimitrakopoulos, K. A. Jenkins, D. B. Farmer, H. Y. Chiu, A. Grill, and P. Avouris, *Science* **327**, 5966 (2010).
- ⁵M. Z. Hasan and C. L. Kane, *Rev. Mod. Phys.* **82**, 3045 (2010).
- ⁶S. Y. Xu, Y. Xia, L. A. Wray, S. Jia, F. Meier, J. H. Dil, J. Osterwalder, B. Slomski, A. Bansil, H. Lin, R. J. Cava, and M. Z. Hasan, *Science* **332**, 560 (2011).
- ⁷J. T. Yates, *Science* **279**, 335 (1998).
- ⁸T. Rakshit, G.-C. Liang, A. W. Ghosh, and S. Datta, *Nano Lett.* **4**, 1803 (2004).
- ⁹B. E. Kane, *Nature (London)* **393**, 133 (1998).
- ¹⁰A. Politi, J. C. F. Matthews, and J. L. O'Brien, *Science* **325**, 1221 (2009).
- ¹¹M. B. Haider, J. L. Pitters, G. A. DiLabio, L. Livadaru, J. Y. Mutus, and R. A. Wolkow, *Phys. Rev. Lett.* **102**, 046805 (2009).
- ¹²T. C. Shen, C. Wang, G. C. Abeln, J. R. Tucker, J. W. Lyding, Ph. Avouris, and R. E. Walkup, *Science* **268**, 1590 (1995).
- ¹³J. W. Lyding, T. C. Shen, J. S. Hubacek, J. R. Tucker, and G. C. Abeln, *Appl. Phys. Lett.* **64**, 2010 (1994).
- ¹⁴S. R. Schofield, N. J. Curson, M. Y. Simmons, F. J. Rueß, T. Hallam, L. Oberbeck, and R. G. Clark, *Phys. Rev. Lett.* **91**, 136104 (2003).
- ¹⁵M. B. Haider, J. L. Pitters, G. A. DiLabio, L. Livadaru, J. Y. Mutus, and R. A. Wolkow, *Phys. Rev. Lett.* **102**, 046805 (2009).
- ¹⁶T. C. G. Reusch, O. Warschkow, M. W. Radny, P. V. Smith, N. A. Marks, N. J. Curson, D. R. McKenzie, and M. Y. Simmons, *Surf. Sci.* **061**, 4036 (2007).
- ¹⁷M. W. Radny, P. V. Smith, T. C. G. Reusch, O. Warschkow, N. A. Marks, H. F. Wilson, S. R. Schofield, N. J. Curson, D. R. McKenzie, and M. Y. Simmons, *Phys. Rev. B* **76**, 155302 (2007).
- ¹⁸M. Dubois, L. Perdigão, C. Delerue, G. Allan, B. Grandidier, D. Deresmes, and D. Stiévenard, *Phys. Rev. B* **71**, 165322 (2005).
- ¹⁹Y. Enta, S. Suzuki, and S. Kono, *Phys. Rev. Lett.* **65**, 2704 (1990).
- ²⁰T. Tabata, T. Aruga, and Y. Murata, *Surf. Sci. Lett.* **179**, L63 (1987).
- ²¹B. Naydenov and J. J. Boland, *Phys. Rev. B* **82**, 245411 (2010).
- ²²J. J. Boland, *J. Vac. Sci. Technol. A* **10**, 2458 (1992).
- ²³Vienna Ab-initio Simulation Package: [<http://cms.mpi.univie.ac.at/vasp/vasp/vasp.html>].
- ²⁴G. Kresse and J. Hafner, *Phys. Rev. B* **47**, 558 (1993).
- ²⁵G. Kresse and J. Hafner, *Phys. Rev. B* **49**, 14251 (1994).
- ²⁶J. P. Perdew, K. Burke, and M. Ernzerhof, *Phys. Rev. Lett.* **77**, 3865 (1996).
- ²⁷J. Tersoff and D. R. Hamann, *Phys. Rev. Lett.* **50**, 1998 (1983).
- ²⁸J. Tersoff and D. R. Hamann, *Phys. Rev. B* **31**, 805 (1985).
- ²⁹B. Naydenov, P. Ryan, L. C. Teague, and J. J. Boland, *Phys. Rev. Lett.* **97**, 098304 (2006).
- ³⁰B. Naydenov, M. Mantega, I. Rungger, S. Sanvito, and J. J. Boland, *Phys. Rev. B* **84**, 195321 (2011).
- ³¹G. A. Shah, M. W. Radny, P. V. Smith, S. R. Schofield, and N. J. Curson, *J. Chem. Phys.* **133**, 014703 (2010).
- ³²E. Hill, B. Freelon, and E. Ganz, *Phys. Rev. B* **60**, 15896 (1999).
- ³³D. R. Bowler, J. H. G. Owen, C. M. Goringe, K. Miki, and G. A. D. Briggs, *J. Phys.: Condens. Matter* **12**, 7655 (2000).